Supporting information

Optimal Sensitizer Concentration in Single Upconversion Nanocrystals

Chenshuo Ma[†,‡], *Xiaoxue Xu*[*,‡,§], *Fan Wang*,[*‡,§], *Zhiguang Zhou*[§], *Deming Liu*[§], *Jiangbo Zhao*[‖], *Ming Guan*[§], *Candace I Lang*[†], *and Dayong Jin*[*,‡,§,⊥]

† Department of Engineering, Faculty of Science and Engineering, Macquarie University, Sydney, NSW, 2109, Australia

‡Advanced Cytometry Laboratories, ARC Centre of Excellence for Nanoscale BioPhotonics, Macquarie University, Sydney, NSW, 2109, Australia

§Institute for Biomedical Materials and Devices (IBMD), Faculty of Science, University of Technology Sydney, NSW, 2007, Australia

‖Institute for Photonics and Advanced Sensing (IPAS) and School of Physical Sciences, University of Adelaide, Adelaide, SA 5005, Australia

⊥ARC Research Hub for Integrated Device for End-user Analysis at Low-levels (IDEAL), Faculty of Science, University of Technology Sydney, NSW, 2007, Australia

*Email: dayong.jin@uts.edu.au.

*Email: fan.wang@uts.edu.au.

*Email: xiaoxue.xu@mq.edu.au.

EXPERIMENT:

1. Materials

$YCl_3 \cdot 6H_2O$ (99.99%), $YbCl_3 \cdot 6H_2O$ (99.99%), $TmCl_3 \cdot 6H_2O$ (99.99%), $GdCl_3 \cdot 6H_2O$ (99.99%), $TbCl_3 \cdot 6H_2O$ (99.99%), $LuCl_3 \cdot 6H_2O$ (99.99%), NH_4F (>98%), NaOH (>97%), oleic acid (OA, 90%), and 1-octadecene (ODE, 99%) were purchased from Sigma-Aldrich and used as received without further purification.

2. Synthesis of hexagonal-phase $NaYF_4$ nanocrystals:

$NaYF_4$ nanocrystals were synthesized using a typical method as previous work. Typically, methanol solution of 0.04 mmol $TmCl_3$, 0.96 mmol YCl_3 were mixed with 6 ml OA and 15 ml ODE in a 50 ml round bottom flask. The mixed solution was heated up to 150 ˚C for 30 min until it became clear. With gentle flow of argon gas through the reaction flask, the solution cooled slowly to room temperature. Methanol solution dissolved with 4 mmol NH_4F and 2.5 mmol NaOH was added into the flask with vigorous stirring for more than 30 min. Then, the mixed solution was heated up to 90 ˚C to evaporate methanol and to 150 ˚C to evaporate all the residual water. Finally, the solution was heated to 300 ˚C in an argon atmosphere and kept at this temperature for 90 min for complete reaction and crystal formation. After reaction and cooling down to room temperature, the synthesized nanocrystals were washed with cyclohexane/ethanol for several times and dispersed in cyclohexane for use. Other $NaYF_4$: 4% Tm^{3+}, *x*% Yb^{3+} (*x*= 20, 30, 45, 60), $NaYF_4$: 4% Tm^{3+}, 20% Yb^{3+}, *y*% Lu^{3+} (*y*= 10, 25, 40, 60), $NaYF_4$: 4% Tm^{3+}, *z*% Tb^{3+} (*z*= 20, 30, 45, 60), $NaYF_4$: 4% Tm^{3+}, 20% Gd^{3+} samples were synthesized as the same route using varied concentrations.

3. Synthesis of hexagonal phase core-shell structure and sandwich structure nanocrystals:

For the synthesis core-shell structure nanocrystals, typically, $NaYF_4$: 60% Tb^{3+}, 4% Tm^{3+} @ $NaYbF_4$: 4% Tm^{3+} nanocrystal. A modified hot-injection method was used for growing shells onto the core nanocrystals. 0.2 mmol $NaYF_4$: 60% Tb^{3+}, 4% Tm^{3+} nanocrystals were dispersed in cyclohexane and mixed with OA (3mL) and ODE (8mL) in a 50mL three-neck flask. The mixture was degassed under Ar flow and kept at 100 ˚C for 30 min to completely remove cyclohexane. Then heated up to 150 ˚C and kept at this temperature for 15 min to remove the any possible water. The mixture solution was quickly heated to 300˚C and $NaYbF_4$: 4% Tm^{3+} source solution was

injected to the core nanocrystals mixture solution using syringe. The injection rate is 0.05 ml/2 min. After the reaction, the precipitate was washed with cyclohexane/ethanol for several times and dispersed in cyclohexane for use. $NaYF_4$: 20% Gd^{3+}, 4% Tm^{3+} @ $NaYbF_4$: 4% Tm^{3+} nanocrystal samples were synthesized as the same route.

For the synthesis sandwich structure nanocrystals, typically, $NaYF_4$: 60% Tb^{3+}, 4% Tm^{3+} @ $NaYbF_4$: 4% Tm^{3+} @ $NaYF_4$ nanocrystal. The $NaYF_4$: 60% Tb^{3+}, 4% Tm^{3+} @ $NaYbF_4$: 4% Tm^{3+} nanocrystals were obtained, and further injection of more $NaYF_4$ source solution by using the same method. $NaYF_4$: 20% Gd^{3+}, 4% Tm^{3+} @ $NaYbF_4$: 4% Tm^{3+} @ $NaYF_4$ nanocrystal samples were synthesized as the same route.

4, Monodispersed single UCNPs samples

1, Place a drop of 50 µl Poly-L-lysine solution (0.1% w/v in H_2O) on a cleaned cover-glass and leave it for 30 mins before rinse it using water and dry the surface at room temperature.

2. Prepare 0.01 mg/ml UCNPs dispersion in cyclohexane, and place a drop of 20 µl UCNPs dispersion onto the cover-glass, then carefully rinse it using cyclohexane and let it dry naturally.

3. Make a drop of 20 µl Embedding Media on a glass slide, and then place the cover-glass onto the glass slide with Embedding media and squeeze out any air bubbles. Then dry the sample in an oven at 60 ˚C.

CHARACTERIZATIONS:

1. TEM Characterization:

The morphology of the synthesize nanocrystals was characterized using transmission electron microscopy (TEM) imaging (Philips CM10 TEM) with an operating voltage of 100 kV. The samples were prepared by placing a drop of a dilute suspension of nanocrystals onto the formvar-coated copper grids (300 meshes) and allowing it to dry in a desiccator at room temperature.

2. XRD Characterization:

Powder X-ray diffraction (XRD) patterns were obtained using a PANalyticalX'Pert Pro MPD X-ray diffractometer using Cu Kα1 radiation (40 kV, 40 mA, λ=0.15418 nm). The XRD samples were prepared by several drops of nanocrystal dispersions in cyclohexane cast on a zero-background silicon wafer.

3. Upconversion photoluminescence spectra by spectrofluorometer:

The upconversion luminescence spectra were obtained using of a Fluorolog-Tau3 spectrofluorometer (JobinYvon-Horiba) equipped with an external 980 nm CW diode laser with a pump power density of 500mW/cm^2. The upconversion nanocrystals were dispersed in the cyclohexane and were prepared to the concentration of 1 mg/ml normalized to the same Tm^{3+} concentration by the subtractive weighting method and inductively coupled plasma mass spectrometry (ICP-MS, Agilent 7500cx ICP-Quadrupole Mass Spectrometer) for the entire specimen. The dispersion was transferred to quartz cuvettes with 10 mm path length and three measurements were conducted for each sample.

4. Photoluminescence characterization of single UCNPs using Scanning Confocal Microscopy:

We built a stage-scan confocal microscope for the intensity measurement of single UCNPs as shown in Figure S9. The excitation source is a 980 nm single mode polarized laser (power density of 30MW/cm^2) which is focused onto the sample through a 100x objective lens (NA 1.4). The emission from sample is collected by the same objective lens and refocused into an optical fiber which has a core size matching with system Airy disk. A Single Photon Counting Avalanche Diode (SPAD) detector is connected to the collection optical fiber to detect the emission intensity. The scanning is achieved by moving the 3D piezo stage.

During the point by point scanning process, when the excitation laser beam moves closer to a single nanocrystal, the system will detect a brighter emission intensity. Therefore each of single nanocrystal will present a Gaussian spot in the confocal scanning microscope image. The maximum brightness value (photon count) of each Gaussian spot can be used to represent the brightness of that single particle. For each confocal image, we record all of the single nanocrystals' brightness values (photon counts). For each batch of samples, we average more than 15 single nanocrystals' values to give a mean brightness with standard deviation as error bars.

SUPPORTING RESULTS

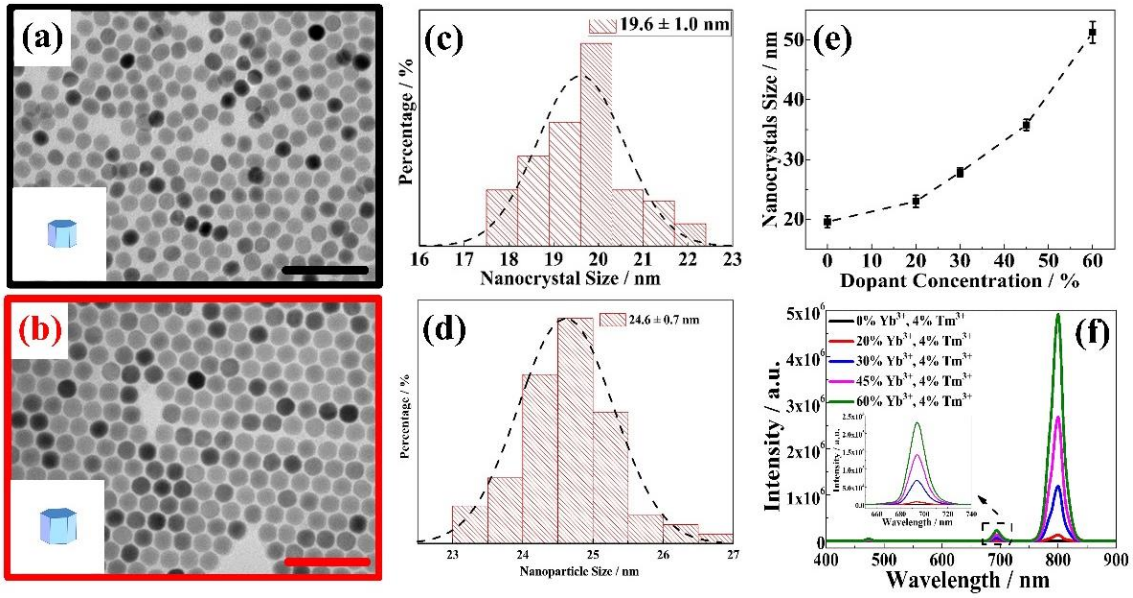

Figure S1.TEM images for $NaYF_4$: 4% Tm^{3+}, *x*% Yb^{3+} nanocrystals (a) *x*=0, (b) *x*=20 and crystal size distribution histograms corresponding to TEM images with (c) 19.6 ± 1.0 nm and (d) 24.6 ± 0.7 nm, respectively, the scale bar is 100 nm. Histograms of the crystals sizes are drawn from analysis of >150 crystals for each sample. (e) point-line curve about the relation between Yb^{3+} doping concentration and nanocrystals size, Yb^{3+}= 0%, 20%, 30%, 45%, 60%. (f) Fluorolog spectrometer measurement of $NaYF_4$: 4% Tm^{3+}, *x*% Yb^{3+} (*x*= 0, 20, 30, 45, 60).

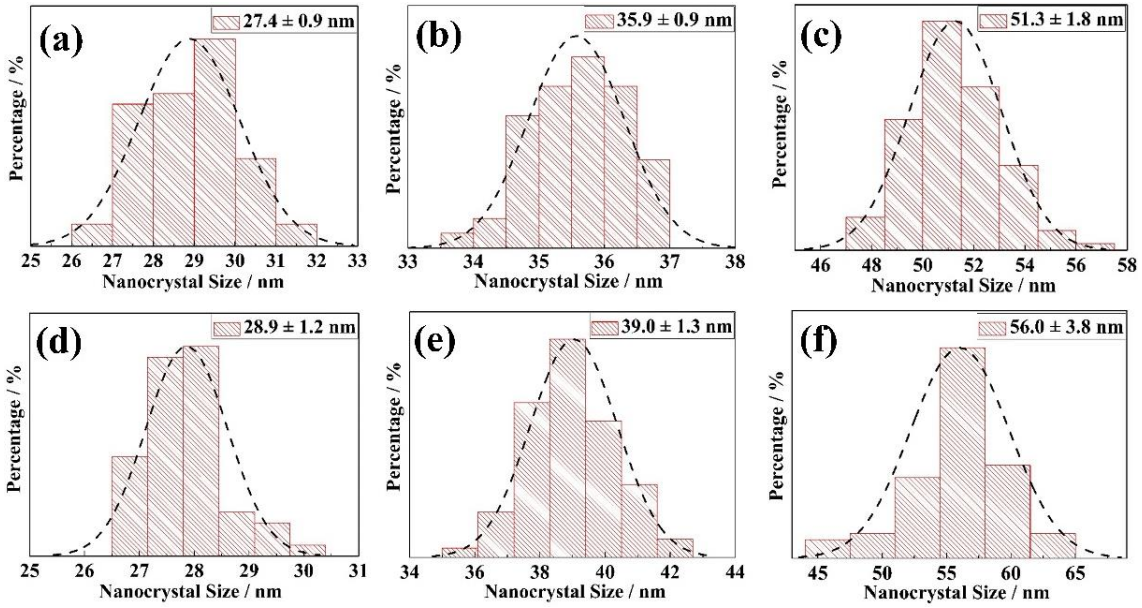

Figure S2. The nanocrystal size distribution histograms corresponding to TEM images in Figure 1a-f, respectively. Histograms of the crystals sizes are drawn from analysis of >150 crystals for each sample. The mean and standard deviation for each monocrystalline diameter are (a) 27.4 ± 0.9 nm; (b) 35.9 ± 0.9 nm; (c) 51.3 ± 1.8 nm; (d) 28.9 ± 1.2 nm; (e) 39.0 ± 1.3 nm; (f) 56.0 ± 3.8 nm, respectively.

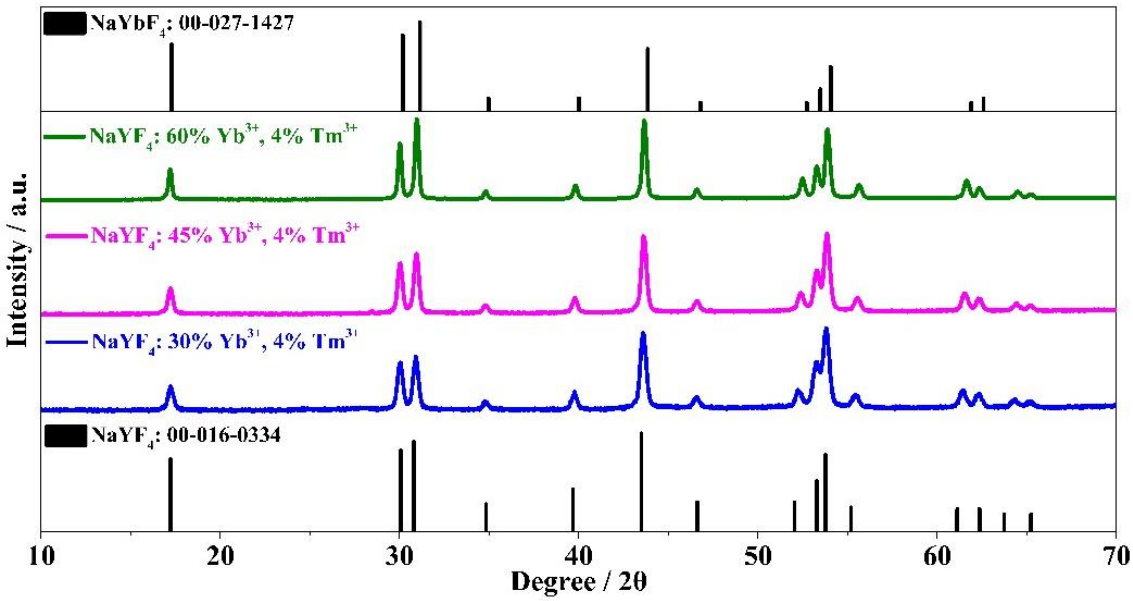

Figure S3. The XRD patterns of $NaYF_4$ nanocrystals co-doped with 4% Tm^{3+} and various concentration of Yb^{3+} ions of 30%, 45% and 60%, respectively, with the standard XRD patterns of hexagonal phase $NaYF_4$ (JCPDS: 00-016-0334) and $NaYbF_4$ (JCPDS: 00-027-1427).

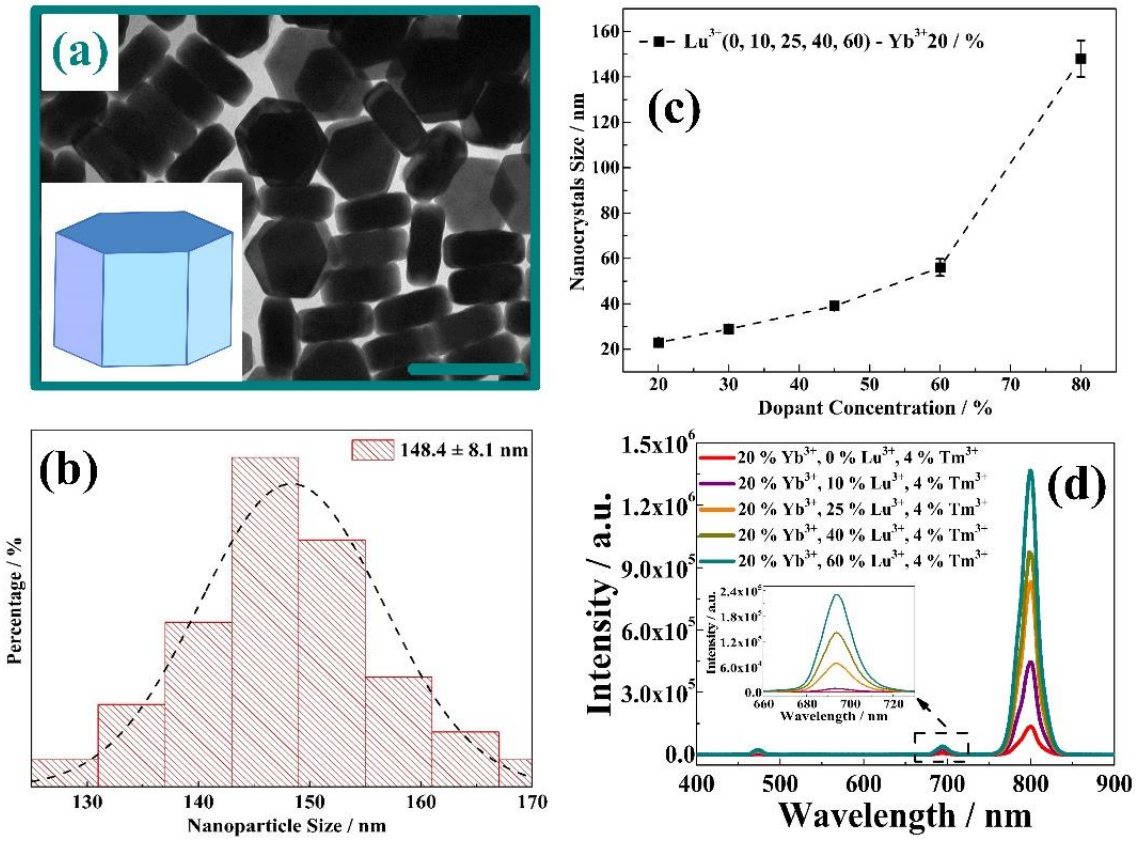

Figure S4. TEM images for (a) $NaYF_4$: 4% Tm^{3+}, 20% Yb^{3+}, 60% Lu^{3+} nanocrystals and crystal size distribution histograms corresponding to TEM images with (b) 148.4 ± 8.1 nm, scale bar is 200 nm. Histograms of the crystals sizes are drawn from analysis of >150 crystals for each sample. (c) point-line curve about the relation between Lu^{3+} doping concentration (Lu^{3+}= 0, 10, 25, 40, 60) and nanocrystals size. (d) Fluorolog spectrometer measurement of $NaYF_4$: 4% Tm^{3+}, 20% Yb^{3+}, *y*% Lu^{3+} (*y*=0, 10, 25, 40, 60).

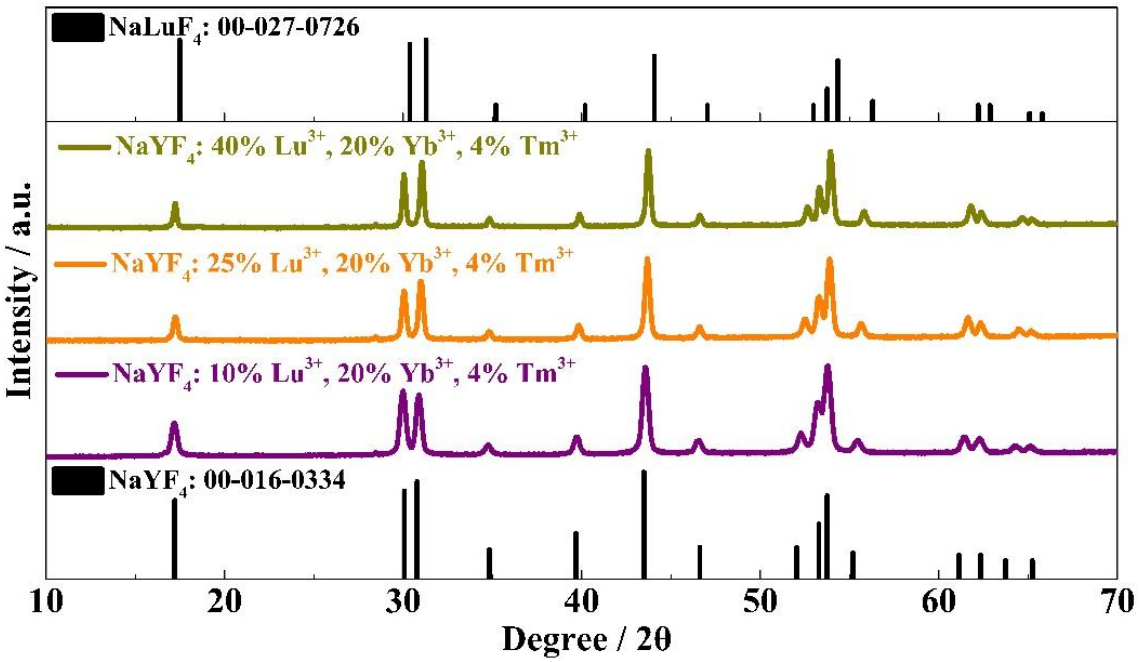

Figure S5. The XRD patterns of $NaYF_4$ nanocrystals co-doped with 4% Tm^{3+}, 20% Yb^{3+} and various concentration of Lu^{3+} ions of 10%, 25% and 40%, respectively, with the standard XRD patterns of hexagonal phase $NaYF_4$ (JCPDS: 00-016-0334) and $NaLuF_4$ (JCPDS: 00-027-0726).

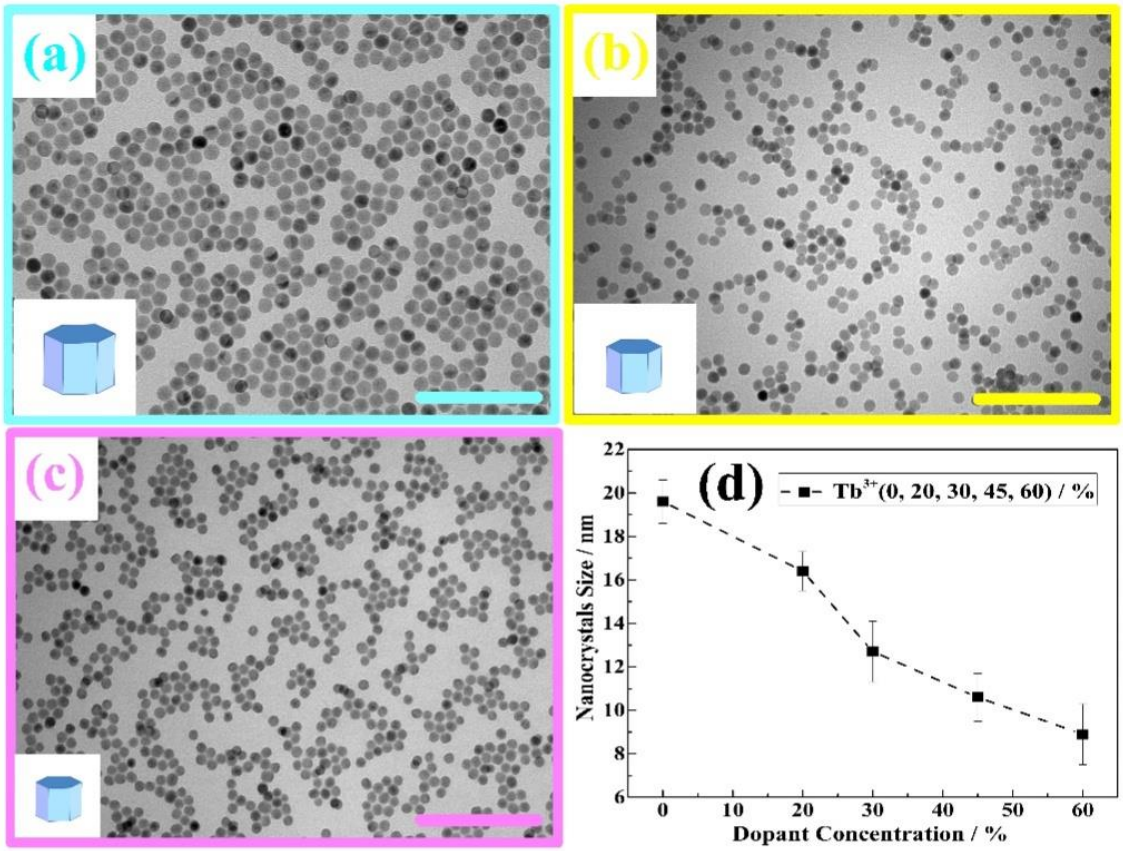

Figure S6. TEM images of different Tb^{3+} concentration β-$NaYF_4$: *z*% Tb^{3+}, 4% Tm^{3+} (*z*= 20, 30, 45) nanocrystals (a) *x*=20, (b) *x*=30, (c) *x*=45, scale bar is 100 nm, and (d) point-line curve about the relation between Tb^{3+} doping concentration (Tb^{3+}= 0%, 20%, 30%, 45%, 60%) and nanocrystals size.

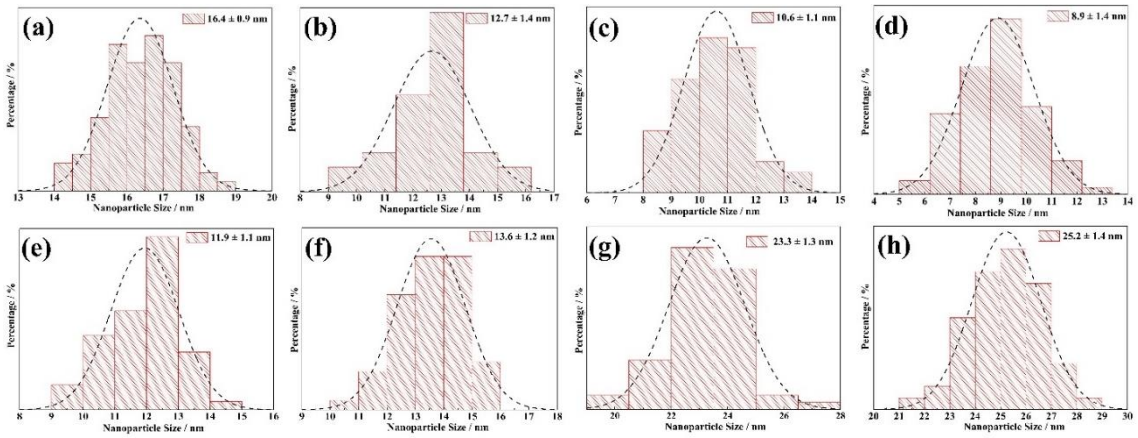

Figure S7. The size distribution histograms of β-$NaYF_4$: x% Tb^{3+}, 4% Tm^{3+} UCNPs corresponding to TEM images in Figure S6a-c for (a) 16.4 ± 0.9 nm; (b) 12.7 ± 1.4 nm; (c) 10.6 ± 1.1 nm, respectively, and Figure 3a for (d) 8.9 ± 1.4 nm. Figure 4b and c for (e) 11.9 ± 1.1 nm, (f) 13.6 ± 1.2 nm; Figure 4e and 4f for (g) 23.3 ± 1.3 nm and (h) 25.2 ± 1.4 nm, respectively. Histograms of the crystals sizes are drawn from analysis of >150 crystals for each sample.

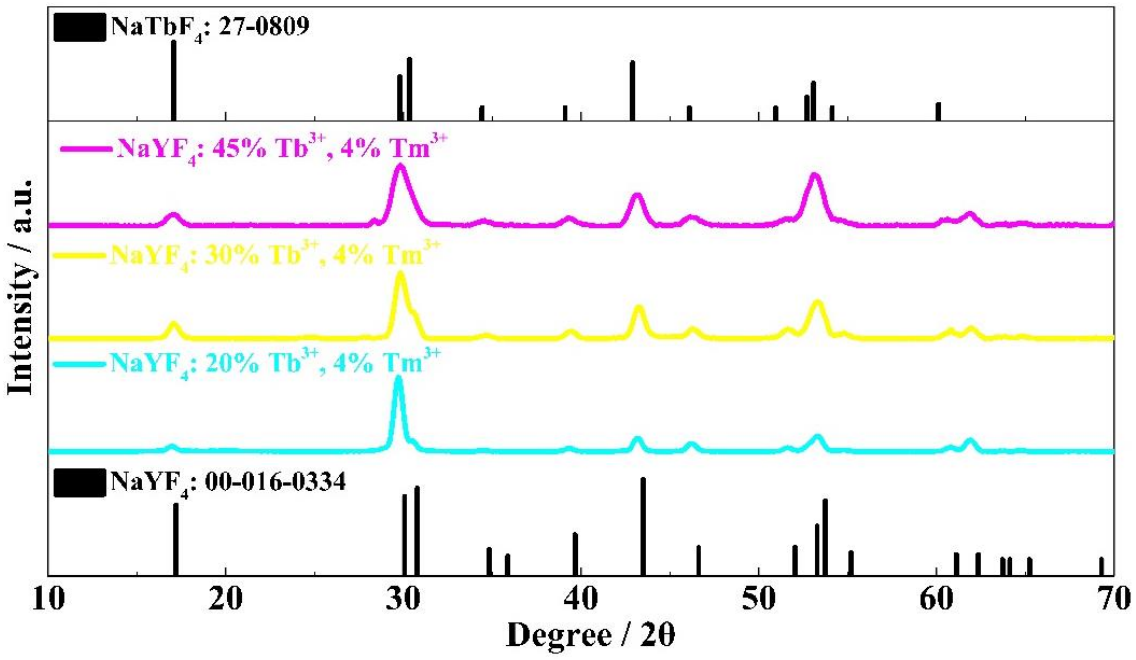

Figure S8. The XRD patterns of $NaYF_4$ nanocrystals co-doped with 4% $Tm^{3+}$and various concentration of Tb^{3+} ions of 20%, 30% and 45%, respectively, with the standard XRD patterns of hexagonal phase $NaYF_4$ (JCPDS: 00-016-0334) and $NaTbF_4$ (JCPDS: 27-0809).

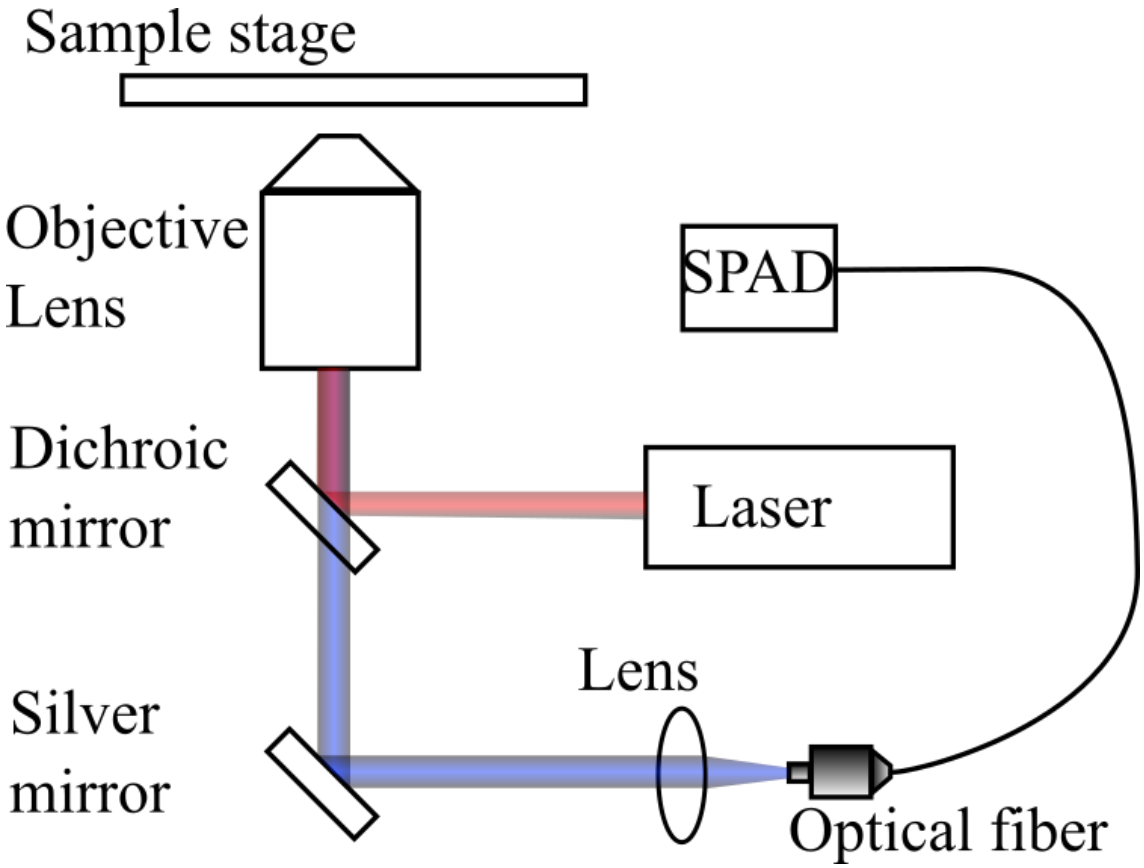

Figure S9. Schematic illustration of the system setup for customized scanning confocal microscope.

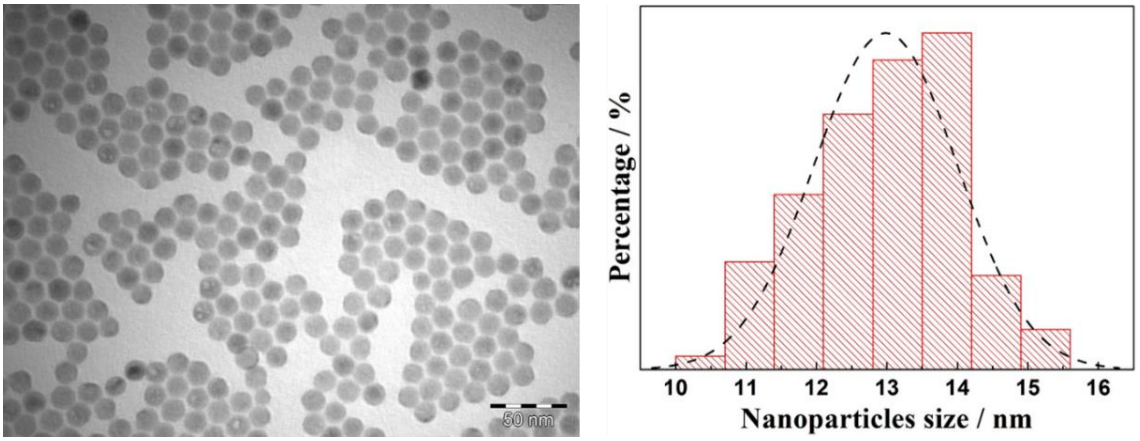

Figure S10. TEM images of β-$NaYF_4$: 20% Yb^{3+}, 4% Tm^{3+} and the size distribution histograms of it corresponding to TEM image, nanocrystals size is 13.0 ± 1.0 nm, scale bar is 50 nm. Histograms of the crystals sizes are drawn from analysis of >150 crystals for the sample.

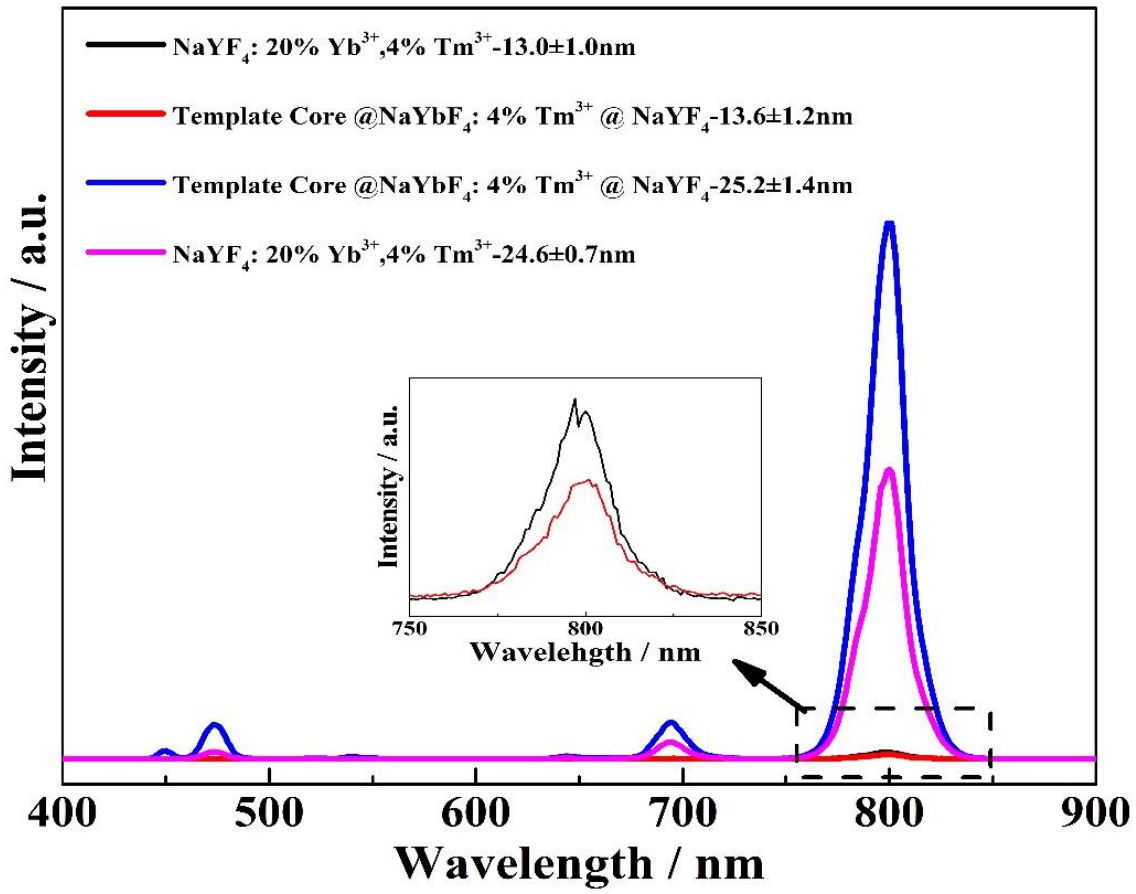

Figure S11. Fluorolog spectrometer measurement of nanocrystals template core @ $NaYbF_4$: 4% Tm^{3+} and template core @ $NaYbF_4$: 4% Tm^{3+} @ $NaYF_4$ structure with different size, and the similar size with $NaYF_4$: 20% Yb^{3+}, 4% Tm^{3+}, respectively.

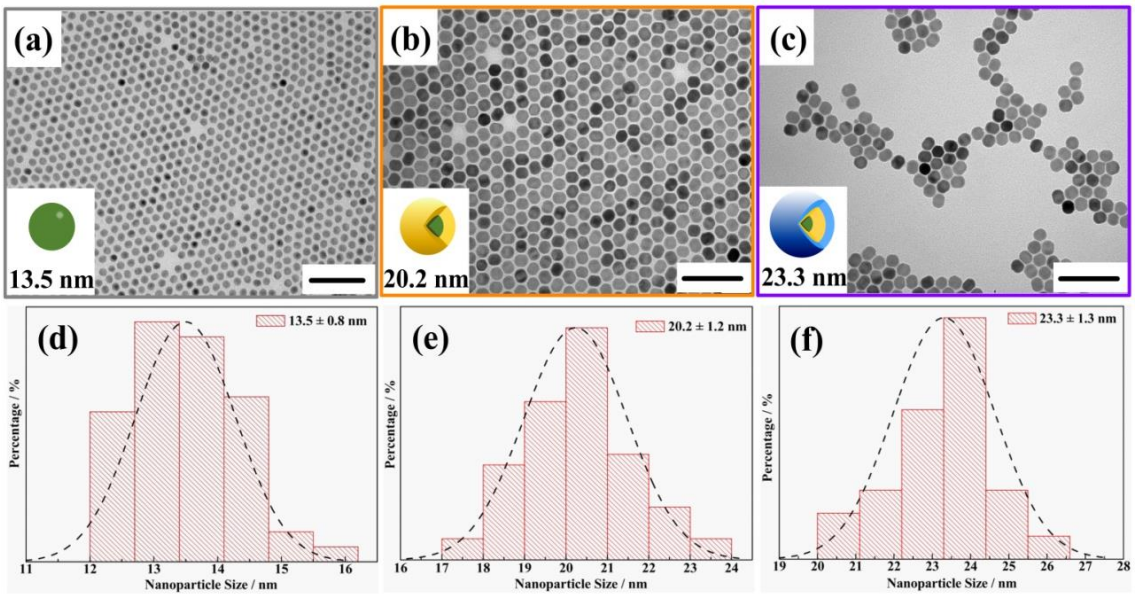

Figure S12. TEM images of (a) template core nanocrystals of $NaYF_4$: 20% Gd^{3+}, 4% Tm^{3+} with the size of 13.5 nm,(b) template core @ active shell nanostructure of $NaYF_4$: 20% Gd^{3+}, 4% Tm^{3+} @ $NaYbF_4$: 4% Tm^{3+} with size of 20.2 nm, (c) template core @ active shell @ inert shell nanostructure of $NaYF_4$: 20% Gd^{3+}, 4% Tm^{3+} @ $NaYbF_4$: 4% Tm^{3+} @ $NaYF_4$ with the size of 23.3 nm, scale bar is 100 nm. (d-f) are the size distribution histograms of their corresponding to TEM images (a-c), respectively. Histograms of the crystals sizes are drawn from analysis of >150 crystals for each sample.

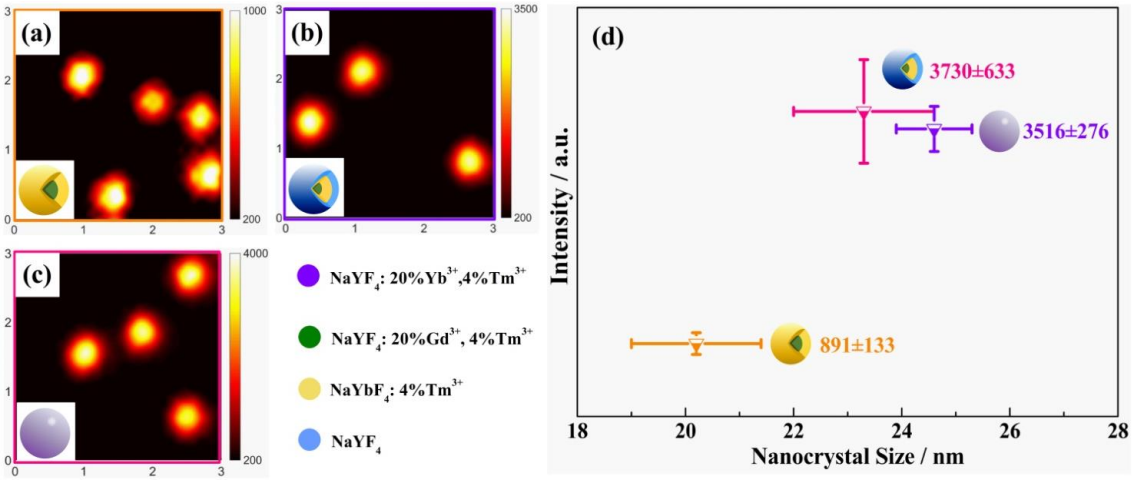

Figure S13. Confocal microscopy quantitative measurement of the whole spectrum emission for single UCNCs: (a) UCNCs of $NaYF_4$: 20% Gd^{3+}, 4% Tm^{3+} core @ active shell of $NaYbF_4$: 4% Tm^{3+} with the size of 20.2 nm, (b) UCNCs of $NaYF_4$: 20% Gd^{3+}, 4% Tm^{3+} core @ active shell of $NaYbF_4$: 4% Tm^{3+} @ inert shell of $NaYF_4$ with the size of 23.2 nm, (c) monolithic UCNCs of $NaYF_4$: 20% Yb^{3+}, 4% Tm^{3+} in size of 24.6 nm, (d) quantitative analysis of the whole spectrum emission intensities for single UCNCs corresponding to (a-c).

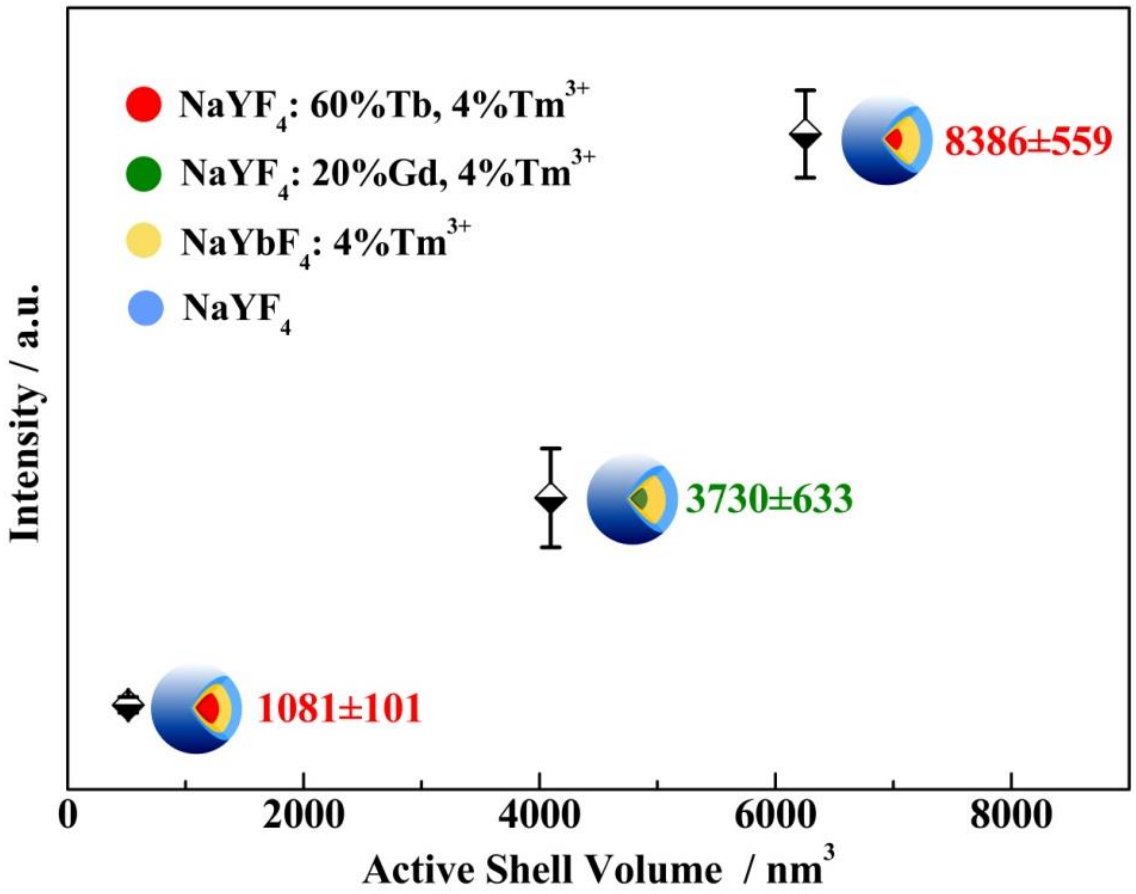

Figure S14. The whole spectrum emission intensities of single UCNCs with different design of sandwich nanostructures show a linear trend following the total volume of active shells.